

The consequent lowering of the triplet energy due to the presence of negative acceptor ions would have the effect mentioned above of decreasing  $4\Delta_e$  as required by the observed increase in  $w_{ep}$ .

In the limit of large  $n_{ex}$  this effect must go over smoothly to the conduction-band scattering observed in degenerate material, so that it would be expected that the over-all effect of negative acceptor ions on the triplet states of the donors must decrease as  $N_a^-$  increases. This would occur as increasing acceptor concentration smooths the potential variation observed at any lattice site. Indeed, the results shown in Figs. 10 and 11 do display an effect of this sort. It can be seen that the line  $w_{ep}(n_{ex})$  for the compensated As(Ge)

and P(Ge) samples is not parallel to the corresponding lines, either for uncompensated Sb(Ge) or uncompensated As(Ge) or P(Ge). The magnitude of  $\Delta w_{ep}$  on compensation is larger at low  $n_{ex}$  (values of  $\lambda$  larger than 5) than at higher concentrations. Because  $w_{ep}$  itself increases with  $n_{ex}$ , the change in the relative magnitude  $\Delta w_{ep}/w_{ep}$  is even more striking.

Another consequence of this increase of  $\Delta w_{ep}/w_{ep}$  as  $n_{ex}$  decreases, is that in the isolated donor-state regime ( $\lambda$  greater than 5) all compensated samples display the same magnitude of  $w_{ep}$ . Whether this is an accidental effect, or whether it corresponds in some fundamental way to the as yet poorly understood insensitivity of  $w_{ep}$  in Sb(Ge) to compensation is still unclear.

## Pair Spectra Involving Si Donors in GaP

T. N. MORGAN, T. S. PLASKETT, AND G. D. PETTIT

*IBM Watson Research Center, Yorktown Heights, New York 10598*

(Received 25 November 1968)

We discuss the preparation of Si-C- and Si-Zn-doped GaP crystals and present an interpretation of their emission spectra in the light of a recent theory of donor states in GaP. We find that the no-phonon peak is weak or absent in Si-Zn and Si-C pair spectra, and that the multiple peaks observed arise from transitions induced predominantly by phonons from the point  $X$  of the Brillouin zone. This interpretation differs from that of a recent paper by Dean *et al.* The energy of the weak no-phonon transition agrees with that calculated from the binding energies and a reasonable Coulomb pair energy, and the phonon energies equal the known values for the TA, LA, and TO phonons at  $X$ . We show that the displacement in energy between a pair peak and one of its phonon replicas may under certain conditions differ from the energy of the phonon emitted.

### I. INTRODUCTION

THE Group-IV element silicon acts as an amphoteric impurity in GaP. It tends to enter the lattice on Ga sites as a shallow donor,<sup>1</sup> but in  $n$ -type material can also occupy a P site as an acceptor.<sup>2</sup> Efficient luminescence from Si-Si (shallow donor-deep acceptor) pairs has been reported by Lorenz and Pilkuhn,<sup>3</sup> and recently Dean *et al.*<sup>4</sup> have identified pair lines and distant pair bands from Si-Zn and Si-C pairs,<sup>5</sup> although the phonon structure of the bands was not understood. The symmetry properties of donor states on Ga sites in GaP have been discussed by Morgan<sup>6</sup> and shown to have a marked influence on the selection rules for radiative transitions, including those of interest in this paper. We

report here photoluminescent studies of GaP ingots which were either undoped or doped with combinations of the impurities S, Si, C, and Zn. We show that the energies and phonon structure of the pair bands are explained in detail by the theory developed in Ref. 6. These results are summarized in Table I.

### II. EXPERIMENTAL

The GaP was prepared by reacting  $\text{PH}_3$  with molten Ga at about  $1150^\circ\text{C}$  in a vertical open-tube system. A 30-g charge of Ga was placed in a pyrolytic BN crucible (1.5 cm in diameter and about 8 cm deep) which fitted closely in a quartz tube. A stream of 10%  $\text{PH}_3$  in Ar gas was injected with a high velocity onto the surface of the molten Ga.<sup>7</sup> The details of the process are described elsewhere.<sup>8</sup> By maintaining the proper temperature profile along the axis of the crucible, the reactor caused a solid polycrystalline ingot to grow at the bottom at a rate of about 1.8 cm/day.

<sup>1</sup> H. C. Montgomery and W. L. Feldmann, *J. Appl. Phys.* **36**, 3228 (1965).

<sup>2</sup> M. Rubinstein, *J. Electrochem. Soc.* **112**, 1010 (1965); F. A. Trumbore, H. G. White, M. Kowalchik, C. L. Luke, and D. L. Nash, *ibid.* **14**, Abstract No. 2 (1965).

<sup>3</sup> M. R. Lorenz and M. H. Pilkuhn, *J. Appl. Phys.* **38**, 61 (1967).

<sup>4</sup> P. J. Dean, C. J. Frosch, and C. H. Henry, *J. Appl. Phys.* **39**, 5631 (1968); (private communication).

<sup>5</sup> To avoid confusion in labeling pair species, we list the elements in the order established by the generic name, donor-acceptor.

<sup>6</sup> T. N. Morgan, *Phys. Rev. Letters* **21**, 819 (1968).

<sup>7</sup> The  $\text{PH}_3$ -Ar gas mixture was supplied by Precision Gas, Linden, N. J.

<sup>8</sup> T. S. Plaskett, presented at the Electrochemical Society Meeting, Montreal, 1968 (unpublished).

TABLE I. Allowed transitions through four of the possible intermediate states in the conduction and valence bands (superscript  $c$  or  $v$ ). The energies in eV of the intermediate electron and hole states above their respective band edges are shown (in that order) in parentheses. Allowed phonons are labeled according to the symmetry of their localized modes, and 0 denotes a no-phonon transition.

Site	State	$\Gamma_{1c}(0,5,0)$	$\Gamma_{15c}(2,6,0)$	$X_5^v(0,3)$
P	$A_1$	0+LA( $A_1$ )	LO+TA+TO( $T_2$ )	0+all
P	$E$	LA( $E$ )	LO+TA+TO( $T_2$ )	0+all
Ga	$T_2$	LA+TA+TO( $T_2$ )	0+all	0+all
Ga	( $A_1$ in second band)	0+LO( $A_1$ )	Mixes with $T_2$ states of first band through $T_2$ combinations of phonons near $\Gamma$ (or $X$ ).	

The spectra appearing in Figs. 1-4 were obtained from these samples by photoluminescence at 2°K. They were excited by a 100-W Hg arc lamp and analyzed by a Perkin-Elmer grating monochromator with an ultimate resolution of  $\sim 0.5$  meV. A photomultiplier having a S20 response served as the detector. The spectra in Figs. 2 and 4 were taken with reduced excitation intensity to accentuate the phonon structure.<sup>4</sup>

The emission from undoped material (see Fig. 1) showed a dominant N line and its replicas from nitrogen contamination, and occasionally a weak S line from sulfur. No obvious pair spectra (which would appear near 2.2 eV) were detected. The source of N and S was traced to the PH<sub>3</sub>-Ar gas mixture. As indicated by Dean *et al.*,<sup>4</sup> the N could be eliminated by using high-purity H<sub>2</sub> rather than Ar as the carrier gas. The S contamination was not great enough to be a problem and was essentially zero in the first few mm of growth. Carbon doping was achieved by mixing  $\sim 0.1\%$  CH<sub>4</sub> with the

Ar gas and, in material containing S, produced S-C donor-acceptor pair spectra. A typical example taken at low-excitation intensity is shown in Fig. 2. Silicon doping was obtained either by adding Si to the Ga prior to synthesis or by synthesizing at temperatures above 1150°C, which resulted in Si contamination from the quartz. Little or no Si was detected by photoluminescence in undoped material synthesized below 1150°C. The two emission spectra from a heavily Si-doped and lightly C-doped (but still  $n$ -type) ingot are shown in Figs. 3 and 4(a). The Si-Zn-doped material used to produce the spectrum in Fig. 4(b) was prepared by diffusing Zn into wafers cut from a Si-doped ingot.

The spectrum in Fig. 1 is from an undoped ingot grown below 1150°C, as described above. The remaining spectra contain donor-acceptor pair bands whose positions depend upon the binding energies and separation of the radiating impurity pairs. This dependence is discussed in Sec. III.

### III. THEORY OF DONOR-ACCEPTOR PAIR BANDS

Hopfield *et al.*<sup>9</sup> first identified the emission from donor-acceptor pairs in GaP and used the discreet pair lines to determine the sums  $E_d + E_a$  of the binding energies of the impurity pairs involved.<sup>10</sup> They based their analysis on the relationship between emission energy  $E$  and pair separation  $R$ :

$$E = E_g - (E_d + E_a) + E_C, \quad (1)$$

where  $E_C$  is the Coulomb energy of the ion pair, and

$$E_C = e^2/KR.$$

Equation (1) is obeyed quite well at large  $R$ . Deviations which occur when  $R$  is not large are discussed by Hopfield<sup>11</sup> and by Lorenz *et al.*<sup>12</sup> Once the band gap  $E_g$

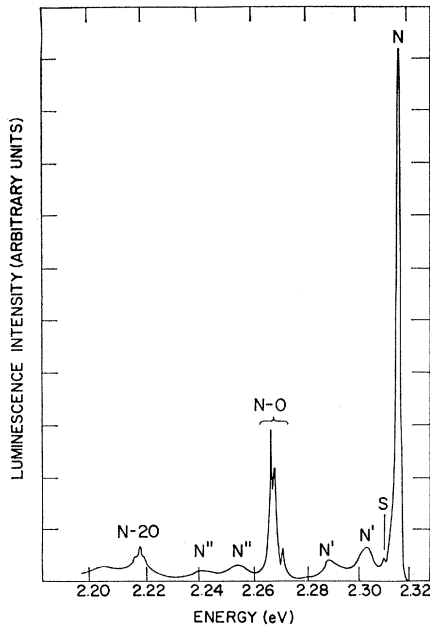


FIG. 1. Photoluminescence spectrum of an undoped GaP ingot. The labels N and S mark the no-phonon emission from excitons bound to nitrogen and sulfur impurities, respectively. Primes identify the phonon replicas except for the prominent optical replicas marked by O.

<sup>9</sup> J. J. Hopfield, D. G. Thomas, and M. Gershenson, Phys. Rev. Letters **10**, 162 (1963); D. G. Thomas, M. Gershenson, and F. A. Trumbore, Phys. Rev. **133**, A269 (1964).

<sup>10</sup> A listing of the currently accepted values of  $E_g$  and the binding energies of C, Zn, S, Te, and Si impurities appears in Table I of Ref. 4.

<sup>11</sup> J. J. Hopfield, in *Proceedings of the International Conference on the Physics of Semiconductors, Paris, 1964* (Dunod Cie., Paris, 1965), p. 725.

<sup>12</sup> M. R. Lorenz, T. N. Morgan, and G. D. Pettit, Proceedings of the International Conference on Semiconductors, Moscow, 1968 (unpublished).

and binding energies are determined, Eq. (1) can be used to identify  $R$  for the pair producing the distant pair bands in which discrete lines cannot be resolved. Thus, Thomas *et al.*<sup>9</sup> concluded that the emission peak in their experiments originated from pairs for which  $R \approx 50 \text{ \AA}$  under intense excitation but shifted to pairs having  $R > 100 \text{ \AA}$  at the lowest intensities.<sup>13</sup> The theory underlying the determination of the peak position has been discussed by Thomas, Hopfield, and Augustyniak<sup>14</sup> and by Lorenz, Morgan, and Pettit.<sup>12</sup> We summarize and extend here the results of Ref. 12.

If the excitation intensity is high enough to keep the pairs always neutral—the “saturated” condition—and the ion density is not large, the emission intensity per unit energy from (distant) pairs of separation  $R$  is

$$I = AR^4 |M|^2. \quad (2)$$

Here the dipole matrix element  $M$  contains the electron-hole overlap integral between the donor and acceptor states and  $A$  is a constant. The value of  $M$  decreases approximately exponentially with increasing  $R$ ,

$$M \propto e^{-R/a_0}, \quad (3)$$

although the exact dependence is determined by the band structure and the depths of the two interacting electron and hole states. The constant  $a_0$  is related to the effective Bohr radius of the more shallow state. Since the conduction-band valleys in GaP are not at  $k=0$ , recombination occurs through a second-order process. The form of  $M$  may depend upon whether crystal momentum is conserved by interaction with an impurity, with one or more phonons, or with both. For this reason no-phonon and phonon-assisted transitions need not reach their peaks for the same value of  $R$ , and the displacement in energy of the phonon replicas is not necessarily an accurate measure of the phonon energy. When  $M$  varies exponentially according to Eq. (3), the peak of (2) occurs at an energy which corresponds to

$$R = 2a_0, \quad (4)$$

and  $I$  equals half its peak value for  $R = 1.04a_0$  and  $R = 3.42a_0$ . This gives for the width of the line

$$\delta E = 1.34E_C, \quad (5)$$

where  $E_C$  is the value of  $e^2/KR$  at the peak.

At very low excitation intensities—or large ion densities—the emission is not limited by the decay rate  $\propto |M|^2$  but by the smaller capture rate, which we can assume is a slowly varying function of  $R$ . Consequently, the (total) emission intensity becomes

$$I \approx A'R^4 e^{(-4\pi NR^{3/3})}, \quad (6)$$

where  $N$  is the density of majority ions, and nonradiative transitions are neglected. The exponential factor in (6)

<sup>13</sup> See also K. Maeda, *J. Phys. Chem. Solids* **26**, 595 (1965).

<sup>14</sup> D. G. Thomas, J. J. Hopfield, and W. M. Augustyniak, *Phys. Rev.* **140**, A202 (1965).

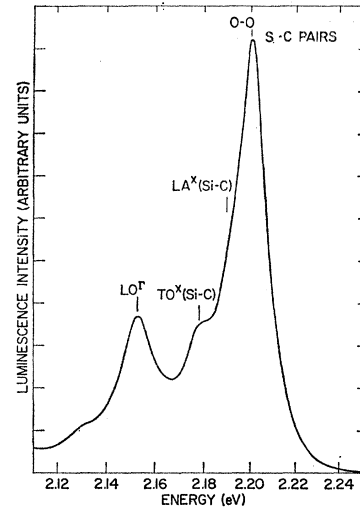


FIG. 2. Photoluminescence spectrum taken at low excitation intensity from a S- and C-doped ingot. The labels identify the no-phonon peak and a replica as well as the position of two peaks from the weak Si-C pair spectrum.

is the probability that a given (minority) ion of a pair has no neighboring (majority) ion nearer than  $R$ .<sup>14</sup> [It has been omitted in Eq. (2).] The exponent equals (minus) the probability that the sphere of radius  $R$  contains one ion. If two or more recombination processes contribute to the total decay rate ( $1/\tau$ ) of a pair state, the emission intensity from one whose partial decay rate is ( $1/\tau_i$ ) equals the total transition rate (radiative and nonradiative) multiplied by the ratio ( $\tau/\tau_i$ ). Thus,

$$I_i = (\tau/\tau_i)I, \quad (7)$$

where  $I$  is given by (2) and (6) in the two limiting cases. The intensity in Eq. (6) reaches its maximum for

$$R = (\pi N)^{-1/3}, \quad (8)$$

which is generally larger than (4), and the linewidth at half-maximum,

$$\delta E = 0.76E_C, \quad (9)$$

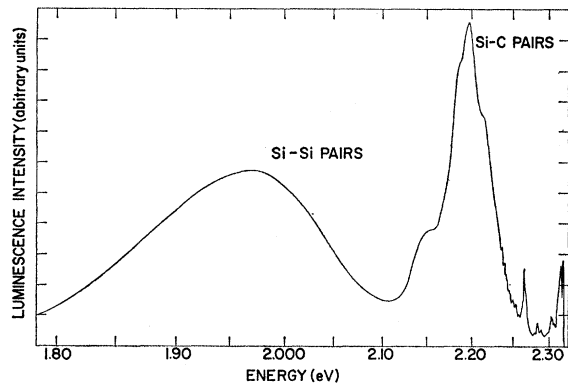
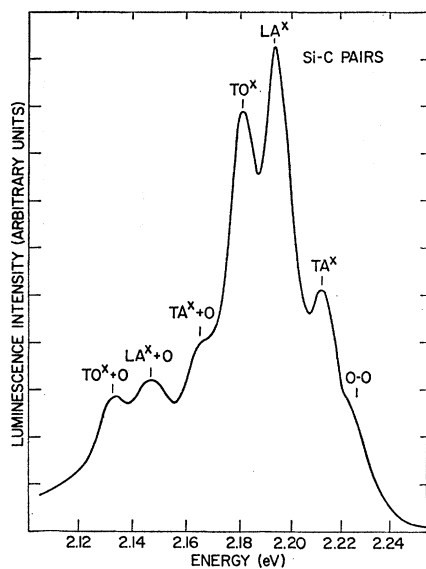
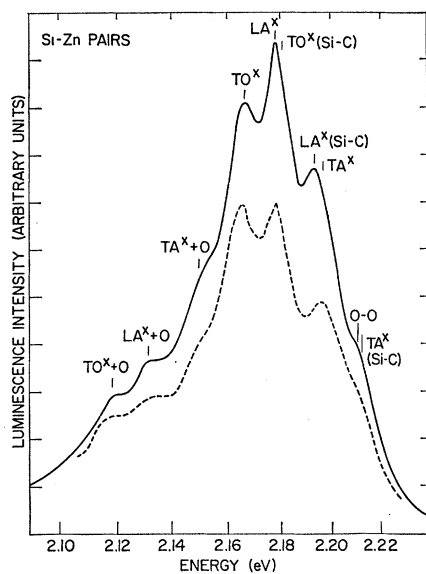


FIG. 3. Photoluminescence spectrum of a heavily Si-doped and lightly C-doped ingot.



(a)



(b)

FIG. 4. Low-intensity photoluminescence spectra of (a) a Si- and C-doped ingot and (b) a Si- and Zn-doped ingot. The phonon replicas are identified. The symbol 0-0 denotes a no-phonon transition, and  $O$  indicates a (local) phonon of  $47 \pm 1$ -meV energy (see text). Peaks from the interfering Si-C spectrum are marked in (b). The dashed spectrum in (b) has been obtained from one of the Zn-doped samples with 5% of the Si-C spectrum (a) subtracted.

is smaller than (5) by 0.57 times the ratio of the values of  $R$  given by (4) and (8). Note that this much smaller half-width provides an explanation of the sharper lines observed at low excitation, as reported in Ref. 4 and shown in our Figs. 2, 4(a), and 4(b). The spectra observed in the laboratory normally lie between these high- and low-intensity limits. Exactly where in this range they lie depends both upon the strength of the

exciting light and upon the nature and numbers of the impurities in the samples. Thus a quantitative comparison of spectra from different samples is difficult.

#### IV. S-C SPECTRUM

The spectrum shown in Fig. 2 is a typical S-C pair spectrum<sup>5,15</sup> taken at low intensity near the unsaturated limit. The peak at 2.201 eV corresponds to no-phonon emission from pairs having  $E_C = 12$  meV and hence  $R \approx 110 \text{ \AA}$ .<sup>10</sup> In this spectrum the shoulder at 2.178 eV and the anomalous linewidth,  $\delta E \approx 1.25E_C$ , are found to be due to Si-C pair emission [Fig. 4(a)] resulting from a small amount of Si contamination. The changes in energy of the two sets of spectra with changes in excitation intensity were generally different and were sensitive to the doping of the samples. In the series of spectra from which Fig. 2 was taken, the Si-C peaks shifted less rapidly than the S-C, while in spectra taken from another part of the same ingot, the opposite was true, and the Si-C spectrum continued to shift as the intensity was reduced below the point where the S-C spectrum had reached its unsaturated limit. A similar S-C spectrum recorded at low intensity appears in Fig. 10 of Ref. 4. The no-phonon peak is also at 2.201 eV,  $E_C = 12$  meV, and the half-width,  $\delta E \approx 10$  meV, satisfies

$$\delta E \approx 0.8E_C.$$

These latter values agree reasonably with (8) and (9) if  $N \approx 2.5 \times 10^{17} \text{ cm}^{-3}$ . In both of these spectra there appear prominent but progressively weaker phonon replicas displaced toward lower energy by multiples of an  $\text{LO}^\Gamma$  phonon energy of  $\sim 50$  meV. In addition, a weaker peak appears in Ref. 4 at  $\sim 28$  meV below the no-phonon peak. This was identified by the authors as a phonon replica, although it also resembles the Si-C peak in our spectrum (Fig. 2), and the 28-meV energy does not agree with any of the phonons which are expected to occur. Although a peak at this energy could be produced by a (very) small amount of Si contamination, the authors have been assured that the 28-meV peak does not arise from this source.<sup>4</sup> Hence, this peak may provide an example of the effect of the phonon-assisted matrix element on peak position (mentioned above). The LA phonon replica, which group theory leads us to expect (see Table I) would appear  $\sim 31$  meV below the no-phonon peak if  $E_C$  were the same in both the no-phonon and phonon-assisted processes. The energy measured by Dean *et al.*<sup>4</sup>—28 meV—lies below this energy by 3 meV, suggesting that the value of  $E_C = 12$  meV for the no-phonon band and its  $\text{LO}^\Gamma$  replica has increased to 15 meV in the  $\text{LA}^x$  phonon replica. Such a shift to higher energy, which corresponds to a smaller value of  $R$ , can occur when the matrix element for the phonon-assisted process decreases more rapidly with

<sup>15</sup> The C was thought to be Si in the early work but is unambiguously identified in Ref. 4 and in the work we report here.

TABLE II. Dependence of electron and phonon symmetries on impurity site. The columns of the periodic table are listed on the right for the common impurities. The decompositions into localized states (for electrons or phonons) are shown at the bottom.

Site	First band	Second band	LA	LO	TA, TO	Donors	Acceptors	Neutral
V (P)	$X_1$	$X_3$	$X_1$	$X_3$	$X_5$	VI	IV	V
III (Ga)	$X_3$	$X_1$	$X_3$	$X_1$	$X_5$	IV	II	III
			$X_1 \rightarrow A_1 + E, X_3 \rightarrow T_2, X_5 \rightarrow T_1 + T_2.$					

increasing pair separation  $R$  than does that for the no-phonon transition. A similarly anomalous phonon energy, 19 meV, was reported by Dean *et al.*<sup>16</sup> in the low-intensity infrared spectra of O-acceptor pairs. We wish here only to suggest the possibility that pair peaks, whose energies are inconsistent with those of the known lattice phonons, may be due to different  $R$  dependences of the relevant matrix elements as well as to local modes. In neither of the two cases considered above has the possibility that the anomalous phonon is a local mode, as the authors suggest, been eliminated. In the former, however, where only shallow impurity states are involved, the appearance of a prominent local mode seems unlikely.

Figure 3 shows a spectrum from a Si-doped crystal containing a small amount of C. The broad Si-Si pair peak at  $\sim 1.96$  eV indicates the presence of Si impurities on both donor (Ga) and acceptor (P) sites.<sup>3</sup> The structured peak near 2.196 eV appears in material doped with both Si and C and is generated by distant Si-C donor-acceptor pairs, as we describe below. This peak, which is repeated at lower excitation intensity in Fig. 4(a), appears to show an entirely different set of phonon replicas from those of Fig. 2. The three peaks at 2.212, 2.194, and 2.181 eV are repeated in a series of phonon replicas  $47 \pm 1$  meV lower in energy. These differences between the S-C and Si-C pair bands, which were noted in Ref. 4, arise because of the different lattice sites occupied by the donors in the two cases. They can be understood in terms of the symmetries of

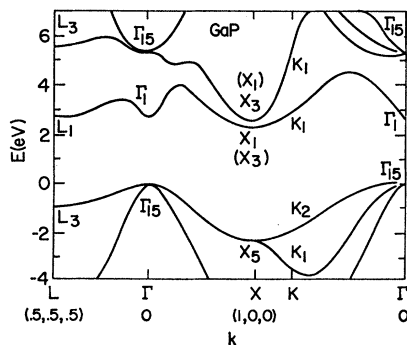


FIG. 5. Band structure of GaP. The conduction-band symmetry at  $X$  for group operations about a P site are shown without parentheses; those about a Ga site appear in parentheses. (Taken from Cohen and Bergstresser, Ref. 17.)

<sup>16</sup> P. J. Dean, C. H. Henry, and C. J. Frosch, Phys. Rev. **168**, 812 (1968).

the electron states involved as noted by Morgan in Ref. 6. We summarize these arguments in Sec. V.

## V. SYMMETRY OF ELECTRON STATES

The conduction-band minima in GaP occur at (or near) the  $X$  points ( $k=2\pi/a$  in the  $x$ ,  $y$ , or  $z$  direction) and lie  $\sim 0.3$  eV below a second set of minima, also at  $X$ . This band structure, as calculated by Cohen and Bergstresser,<sup>17</sup> is shown in Fig. 5. The wave functions associated with these minima are periodic of period  $a=5.45$  Å in the  $x$ ,  $y$ , or  $z$  direction, and each concentrates its maximum probability density on either the P or Ga sublattice. The wave functions change sign between adjacent P or Ga planes. Since the pseudopotential is more attractive (negative) for electrons on P than on Ga, electrons in the lower minima are concentrated on P sites, as indicated in Fig. 6. Those in the higher minima are concentrated on Ga sites. The symmetry of either set of functions depends upon the choice of origin used in defining the group operations. The lower band is found to possess symmetry  $X_1$  if the origin is on a P site, and symmetry  $X_3$  if the origin is on a Ga site. These symmetry assignments are interchanged for the higher band (see Table II).

The symmetry of an electron bound to an impurity can be treated most simply in a coordinate system whose origin coincides with the impurity. Hence, the location of a donor on a Ga site fixes as  $X_3$  the symmetry of the

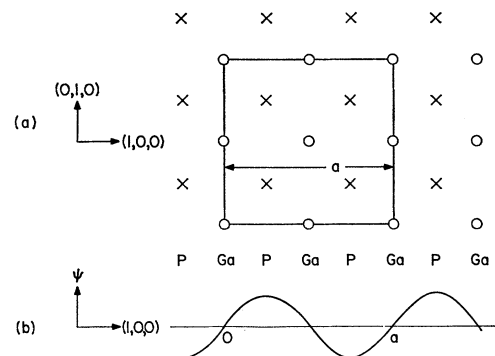


FIG. 6. (a) Projection onto the (001) plane of the atom sites of the (fcc) GaP lattice. (b) The envelope of an electron wave in the conduction-band minimum at  $\mathbf{k}=(1,0,0)(2\pi/a)$ . This function, which vanishes at the Ga sites, has symmetry  $X_3$  about a Ga and  $X_1$  about a P site.

<sup>17</sup> M. L. Cohen and T. K. Bergstresser, Phys. Rev. **141**, 789 (1966).

conduction-band minima about that site and identifies the representation to which the three degenerate donor states belong as  $T_2$ . The electron wave functions in these states vanish at the impurity site and interact only weakly with the core potential. Similarly, the electron states in the higher minima transform as  $X_1$  and have their threefold degeneracy split by the impurity potential into a nondegenerate  $A_1$  state and a twofold set of  $E$  states. These assignments would be interchanged for a donor on a P site.

Since the Si donors occupy Ga sites, the bound electron states transform as  $T_2$  and are weakly mixed by the donor impurity potential with  $T_2$  ( $\equiv \Gamma_{15}$ ) states or combinations of states elsewhere in the Brillouin zone. Consequently, in donor-acceptor pair spectra involving Si donors and distant shallow (Zn or C) acceptors, the no-phonon line is weak or absent and derives what strength it has from coupling between the  $X_3$  and  $\Gamma_{15}$  conduction-band states and between the  $\Gamma_{15}$  and  $X_5$  valence band states (see Table I). Since this latter mixing depends on the interaction between the acceptor potential and the holes, it is greatest when the acceptor is deep and occupies a Ga site, as for Zn. Somewhat stronger no-phonon emission is possible from close-spaced pairs, since the perturbing acceptor potential relaxes the selection rules for transitions between conduction-band states.

Although no-phonon transitions between the distant pairs are only weakly allowed, radiative transitions can occur readily with the cooperation of (predominantly)  $X$ -point phonons which have the proper symmetry, since they satisfy the  $k$ -selection rule for transitions between the unperturbed (band) states. The strongest transitions occur through the nearby  $\Gamma_1$  conduction-band minimum and require an  $X$  phonon which transforms as  $T_2$ . As noted in Table II, which is reproduced from Ref. 6, for an impurity on a Ga site, these are the LA, TA, and TO modes.<sup>18</sup> Additional transitions which involve any of the  $X$  phonons can occur through the  $\Gamma_{15}$  states in the conduction band or the  $X_5$  points of the valence band (see Table I), though their strength is reduced because of the large energy differences between the states. Of the four phonon modes at  $X$ , the transverse modes involve motion of both sublattices of the crystal, whereas the longitudinal modes involve out-of-phase motion of adjacent  $\langle 100 \rangle$  planes of only the Ga (LA) or P (LO) atoms, while the other sublattice remains at rest. For this reason the strength of coupling to either of the longitudinal modes can depend upon whether the impurity ions occupy Ga or P sites.

Since the S donors occupy P sites, they bind electrons in singlet states which transform as  $A_1$  ( $\equiv \Gamma_1$ ) and are mixed with the  $\Gamma_1$ ,  $k \approx 0$  conduction-band states by the impurity potentials. Thus, pair emission occurs readily through the  $\Gamma_1$  conduction band either without phonon

emission or with emission of an LA phonon (see Table I). In addition, the LO phonon at  $\Gamma$  can produce an intravalence band coupling which generates a series of replicas separated by about 50 meV.

## VI. INTERPRETATION OF Si SPECTRA

From the above discussion we predict that the no-phonon peak in the Si-C spectrum of Fig. 4(a) should be weak, but that replicas of this "forbidden" transition should occur for band-edge ( $X$ ) phonons. The  $LO^X$  phonon replica should be the weakest. Since the binding energies determined for Si and C are<sup>4</sup>  $E_d = 81$  meV and  $E_a = 48$  meV, the pair peaks should occur at

$$E_i = E_\infty + E_C - \hbar\omega_i, \quad (10)$$

with  $E_\infty = 2.210$  eV and  $E_C$  evaluated at the intensity maximum of the peak. Here  $\hbar\omega_i$  represents the energy of the emitted phonon(s). Since  $E_C$  in Eq. (10) is determined by the  $R$  dependence of the overlap matrix element [see Eq. (2)], its value need not be the same in a phonon-assisted transition, as it is in a no-phonon transition and may depend upon the type of phonon involved. Hence, as noted above, the displacement of a phonon replica of a pair band from the no-phonon band need not equal the energy of the phonon (and the difference may vary with the excitation intensity).

The structure in the spectrum of Fig. 4(a) is found to be described by Eq. (10), with

$$E_C = 15 \text{ meV.}$$

The weak shoulder at 2.225 eV coincides with the expected position of the no-phonon band, and the three prominent peaks at 2.212, 2.194, and 2.181 eV correspond to phonon energies of  $\hbar\omega = 13, 31, \text{ and } 44$  meV. These agree well with the energies found for  $X$ -point phonons by Yarnell *et al.*<sup>19</sup> by neutron spectroscopy. These are  $\hbar\omega = 13.2, 30.9, \text{ and } 43.8$  meV for the TA, LA, and TO branches, respectively. Thus, a single value of  $E_C$  explains the location of all three peaks, suggesting that the important intermediate states are similar in all three cases. As predicted, the 45.4-meV LO branch is not evident, though it might be difficult to distinguish from the TO branch. As noted above, the remaining structure in Fig. 4(a) involves a second broad phonon of energy,  $47 \pm 1$  meV. The Si-C peak in Fig. 3 is similar though shifted to higher energy by 2 meV and broadened because of the higher intensity of the exciting light used.

It has been suggested by Brodsky<sup>20</sup> that the 47-meV phonon is a local mode involving the light Si donor on a Ga site. The predictions of this model are found to be in excellent agreement with experiment. The energy is almost exactly what the model predicts if the force constant remains unchanged, i.e., the motion of a Si

<sup>18</sup> In Table II of Ref. 6, the two transverse phonons were inadvertently omitted from the third ( $\Gamma_1$ ) column for the  $T_2$  state on a Ga site.

<sup>19</sup> J. L. Yarnell, J. L. Warren, R. G. Wenzel, and P. J. Dean, Proceedings of the International Conference on the Inelastic Scattering of Neutrons, Copenhagen, 1968 (unpublished).

<sup>20</sup> M. H. Brodsky (private communication).

atom (atomic weight 28) relative to the nearly stationary surrounding P atoms (atomic weight 31) resembles the  $LA^X$  and  $LO^X$  modes (for which the adjacent atoms are stationary) and should occur at a frequency equal to (or slightly higher than) the square root of the P-to-Si mass ratio times the  $LO^X$  frequency:

$$\hbar\omega_{Si} \gtrsim (31/28)^{1/2} \times 44 = 46.3 \text{ meV}.$$

Its symmetry will be  $T_2$  since it transforms as  $x$ ,  $y$ , or  $z$  about the Ga lattice site. Such a mode will be broadened through coupling to the resonant LO phonon at about the midpoint between  $\Gamma$  and  $X$ . Since a highly local mode contains  $k$  values which span the entire Brillouin zone, it couples most strongly through those intermediate states which lie lowest in energy—the conduction-band minima at  $X$ . Coupling to the next higher states, the second set of minima at  $X$ , is reduced by the square of the ratio of the energy differences, or

$$\sim (0.047/0.345)^2 = 0.02.$$

Hence, this phonon does not appear in a one-phonon transition but does occur as a second phonon in combination with each of the three  $X$  phonons identified above. The transition  $T_2 \times T_2 \rightarrow T_2$  is, of course, allowed.

The Si-Zn spectrum of Fig. 4(b) is similar to the Si-C spectrum of Fig. 4(a) but differs because of: (1) the  $\sim 16$ -meV greater binding energy of the Zn, (2) the change of the acceptor from a P to a Ga site, and (3) the change in mass defect between the impurity and the atom it replaces. The increase in binding energy shifts the emission peaks toward lower energy and increases the strengths of the transitions, including the no-phonon transition, through the  $X_5$  valence-band extrema. The change of the acceptor site also increases the coupling to the hole and, together with the change in mass defect, modifies the relative strengths of the phonon replicas. The Si-Zn-doped material also contained a small amount of C. Hence some of the Si-C pair spectrum appears in Fig. 4(b) and makes difficult an accurate determination of the energies of the Si-Zn peaks. The dashed curve in Fig. 4(b) has been obtained from a

similar Si-Zn spectrum by subtracting 5% of the Si-C spectrum of Fig. 4(a). The peaks of this curve can be fit by Eq. (10) with  $E_{\infty} = 2.194$  eV,  $E_C = 15$  meV, and  $\hbar\omega = 13, 31$ , and  $44$  meV, as before. The no-phonon band appears as a high-energy shoulder near 2.209 eV. Thus again, a single value of  $E_C$  is found to explain the data. The spectra of Fig. 10 in Ref. 4 are similar to our Fig. 4 (as corrected), although no shoulder attributable to a no-phonon transition is evident in the former.

The identification of the high-energy shoulders in Figs. 4(a) and 4(b) as the no-phonon bands is not unambiguous, since an alternate interpretation is possible. These shoulders could be replicas produced by near zone center (acoustic) phonons which, as discussed in Ref. 6, connect the  $T_2$  donor states with  $A_1$  states associated with the second (higher) conduction-band minima. Since these transitions proceed through different sets of intermediate states whose matrix elements may depend differently on  $R$ , the appropriate value of  $E_C$  could be several meV larger than the 15 meV found for the major peaks above, and the peaks could occur at the energies expected for the no-phonon bands.

## VII. CONCLUSIONS

Thus, we have shown that the phonon structure of the Si-C and Si-Zn pair bands is in excellent agreement with the theoretical predictions of Ref. 6, based on the symmetry properties of the donor states. We find that, in agreement with theory, essentially all of the emitted light appears in the TA, LA, and TO phonon replicas of the forbidden no-phonon, line though with some additional emission in a second set of replicas lying  $47 \pm 1$  meV lower in energy. The phonon producing this second set is tentatively attributed to a local mode of the Si donor. The line shapes and positions of the peaks have been analyzed and found to be consistent with the theory of pair emission.

## ACKNOWLEDGMENTS

The authors are grateful to Dr. M. R. Lorenz for helpful discussions and suggestions and to A. H. Parsons for assistance in preparing the material.